

Supporting Information

## **Shedding Light on Azopolymer Brush Dynamics by Fluorescence Correlation Spectroscopy**

R. H. Kollarigowda,<sup>a,b,c,†</sup> I. De Santo,<sup>a,b,†</sup> C. Rianna,<sup>a,b,d</sup> C. Fedele,<sup>a,b</sup> A. C. Manikas,<sup>a,e</sup> S. Cavalli\*<sup>a</sup> and P. A. Netti\*<sup>a,b</sup>

<sup>a</sup> Center for Advanced Biomaterials for Healthcare, Istituto Italiano di Tecnologia, Largo Barsanti e Matteucci 53, 80125, Naples, Italy.

<sup>b</sup> Dipartimento di Ingegneria Chimica dei Materiali e della Produzione Industriale, DICMAPI, Università degli Studi di Napoli Federico II, Piazzale Tecchio 80, 80125, Napoli, Italy.

<sup>c</sup> Current affiliation: National Institute for Nanotechnology (NINT), Department of Chemical and Materials Engineering, University of Alberta, 11421 Saskatchewan Drive, Edmonton, Alberta, Canada

<sup>d</sup> Current affiliation: Institute of Biophysics, University of Bremen, Otto-Hahn Allee, D-28359 Bremen, Germany

<sup>e</sup> Current affiliation: Institute of Chemical Engineering Sciences, Foundation of Research and Technology-Hellas (FORTH/ICE-HT), Stadiou Str., Platani, GR-26504 Patras, Hellas, Greece.

## Table of Contents

Table S1	Synthetic conditions and thickness of polymer brush samples (pMAb)	p. 8
Scheme S1	Synthesis of DR-amine	p. 8
Table S2	Conditions for azo-pMAb 2a and 2b	p. 9
Scheme S2	Synthesis of azo-pMAb 2a and 2b	p. 9
Scheme S3	Synthesis of pMAb 3	p. 10
Figure S1	UV/Vis calibration curve	p. 10
Figure S2	GPC chromatogram of non grafted polymer (pMA)	p.11
Figure S3	2D DOSY-NMR of non grafted polymer (pMA)	p. 11
Figure S4	AFM images of pMAb samples	p. 12
Figure S5	AFM images of silanised (sample 1) and RAFT immobilised (sample 2) glass samples	p. 12
Figure S6	Spectroscopic ellipsometry raw data of azo-pMAb 1 in dry and in wet.	p. 13
Figure S7	XPS of pMAb	p. 13
Figure S8	Contact angles of different glass samples	p. 14
Figure S9	Biocompatibility essay	p. 14
Figure S10	ACF plots of azo-pMAb 1 excited at different wavelength	p. 15
Figure S11	UV/Vis absorption spectrum of azo-pMAb 2a	p. 15
Figure S12	UV/Vis absorption and Raman spectra of azo-pMAb 2b	p. 16
Figure S13	Count rates of azo-pMAb 2a excited with different laser power	p. 16
Figure S14	Number of molecules (N) of azo-pMAb 2a and Rhodamine 6G in solution	p. 17
Figure S15	Confocal Image and ACFs of pMAb 3	p. 17

**Synthesis of DR-amine (compound a in Scheme S1).** 0.32 mmol (100 mg) of *N*-Ethyl-*N*-(2-hydroxyethyl)-4-(4-nitrophenylazo)aniline (Disperse Red 1, here called as DR) was dissolved in 10 ml of dichloromethane (DCM). 0.77 mmol (2.4 equiv., 88.20 mg) of methanesulfonyl chloride and 0.96 mmol (3 equiv., 133  $\mu$ l) of triethylamine (TEA) were added drop wise at 0 °C and the reaction was stirred for 30 minutes at room temperature. The product was confirmed by thin layer chromatography (TLC). The mixture was washed with a saturated solution of bicarbonate, then extracted with DCM and washed again with saturated sodium chloride solution. Finally, the DCM layer was dried over sodium sulfate and filtered. The DCM was evaporated to get a fluffy red powder. Crude product was used directly for the next step without further purification. The obtained intermediate product was reacted for 2 hours with 0.64 mmol (2 equiv., 41.61 mg) of sodium azide in 1.5 ml of DMF at 85 °C. The product was purified by column chromatography by using toluene as eluent. MS for  $C_{15}H_{17}N_7O_2$ : calculated for  $[M+H]^+ = 339.14$  m/z, found (ESI)  $[M+H]^+ = 339.14$  m/z. 0.27 mmol (90 mg) of the desired product was reacted with 0.40 mmol (1.5 equiv., 105 mg) of triphenylphosphine in a mixture of water/tetrahydrofuran (THF) 35/65 (v/v) at room temperature for 24 hours. The reaction was followed by TLC. The THF was evaporated and the product was extracted with DCM. The DCM layer was washed with a saturated bicarbonate solution and a saturated solution of sodium chloride. Finally, the combined DCM layers were dried over sodium sulfate and filtered. The DCM was evaporated to get a fluffy red powder. Further, purification of the product was done by column chromatography with a mixture of methanol/dichloromethane 8/92 (v/v). MS for  $C_{15}H_{19}N_5O_2$ : calculated for  $[M+H]^+ = 313.15$  m/z, found (ESI)  $[M+H]^+ = 313.15$  m/z.

### **Synthesis of azo-pMAb 2.**

*Preparation of azo-pMAb 2a.* The sample was prepared accordingly to the experimental section described for azo-pMAb 1 (until step d in Scheme 1 main text).

*Preparation of azo-pMAb 2b.* The sample was prepared accordingly to the experimental section described for azo-pMAb 1 of the main text until step d in Scheme 1 (main text), applying the following modification to the procedure: glass substrate pMAb after thionyl chloride reaction was washed with tetrahydrofuran and dried under nitrogen flow, then the substrate was placed in 25 ml

corning flask and a solution of 1 equiv. of compound **a** (DR-amine) in 5 ml of DMF was added. After 12 hours 70% of DR grafting was achieved.

For both samples (azo-pMAb 2a and 2b), the quantification of DR on polymer brushes was obtained by UV measurements as described in the experimental section and in Figure S1.

**Synthesis of pMAb 3.** Glass substrate with pMAb were transferred into a 50 ml corning flask. A solution of 1.5 mmol (125  $\mu$ l) of propylamine in 20 ml of DMF was added and the reaction was left shaking on an oscillating plate for 3 hours. 1.5  $\mu$ mol (1 mg) of maleimide-Cy5 was added and the reaction was continued for 24 hours at room temperature. After 24 hours the glass substrate was washed with DMF for 30 minutes with shaking and the washing process was repeated for 5 times to remove unreacted maleimide-Cy5. Finally, glass substrate was immersed in DMF for 24 hours and then washed with acetone and dried in a vacuum oven for 2 hours at 30 °C.

**UV/Vis Spectrophotometry.** UV/Vis absorption was measured on polymer brushes with a UV CARY 100 scan spectra photometer (VARIAN, Australia). Polymer brush sample was mounted with the help of a custom-made 3 cm-long paper holder. Data intervals of 1 nm and a scan of 600 nm/min were used. The base line was corrected by using bare glass. Data were recorded from 200 to 800 nm (glass absorption was until 350 nm). The maximum UV absorption peak for the polymer brushes was observed at 482 nm. After exciting 200 seconds by using FCS, no change in the absorption was observed.

**Gel permeation chromatography.** GPC analysis was done on polymer samples using milliQ water on a Yarra 3 $\mu$ m SEC 200 (300 x 7.8 mm) column and an ELS detector. A flow rate of 1 ml/minute and a pressure of 80 PSI were used. Three poly(MA standards (Sigma-Aldrich) were used for calibration.

**2D DOSY NMR measurements.** Typically, 1 mg of sample was dissolved in 700  $\mu$ l of D<sub>2</sub>O. <sup>1</sup>H and <sup>1</sup>H detected DOSY experiments were performed at 300 K on a Agilent DD2 NMR spectrometer operating at 600 MHz and equipped with a Agilent multinuclear z-gradient inverse one probe head capable of producing gradients in the z direction with a strength of 55 G cm<sup>-1</sup>. In this experiment, Stokes-Einstein equation was applied for estimating the value of diffusion coefficient (D) for molecular species in aqueous solutions:  $D = kT/6\pi\eta R_h$ , where  $K$  is the Boltzmann constant in J/K,  $T$  is the absolute temperature in K,  $\eta$  is the viscosity of the solution in N s m<sup>-2</sup> and  $R_h$  is the hydrodynamic

radius in m. The linear correlation between the diffusion coefficient determined by DOSY and molecular weight was originally noted by Johnson via the equation  $D = k [M]^\alpha$ . Where D is the diffusion coefficient, while k and  $\alpha$  are the partition coefficients of poly(MA) in water.

**AFM technique.** AFM measurements were performed on polymer brush substrates with a JPK AFM Nanowizard. Commercial tips (Bruker) with a resonance frequency of 50 kHz and a spring constant of 0.10 N/m, were used to scan in contact mode all over the samples.

**Ellipsometry.** Spectroscopic ellipsometry measurements were performed with a Nano film ep3SE instrument (Accurion, Germany) equipped with a He-Ne laser ( $\lambda = 658$  nm) and a spectroscopy lamp (Xe arc) for multiple-wavelength spectra. Ellipsometry measures the changes in polarisation that occur upon reflection of a light beam from a sample, typically a thin film deposited upon a reflective substrate. The changes in polarisation depend upon the thickness and the refractive index of the composite layers. These features are not measured directly, but calculated from model fitting of the optical parameters,  $\Delta$  and  $\Psi$ , which are related to the changes in polarisation of the surface structure of the sample. Ellipsometry measurements were conducted in air configuration at fixed temperature of 25 °C. Measurement was carried out using a xenon lamp with a 5x objective and focusing in the region of interest (ROI) of 55° and measuring the angle of incidence (AOI) of 50°- 60°. A step of 0.5°, a polarizer of 50°, a compensator of 45°, an analyzer of 30° and a refractive index for transparent glass of 1.474 were used to fit data. Calculated thickness for all polymer brush samples varied from 150 to 200 nm. For ellipsometry measurements in the wet state a solid/liquid cell was used. In this configuration, spectroscopic ellipsometry has to be performed, fixing the angle of incidence to 60°, while changing wavelength value between 569 and 1001 nm, outside the absorption region of the azopolymer. First of all, measurements were carried out in three regions of interest (ROI) in dry conditions and then after 2 hours in water. Results are reported as raw data..

**X-Ray Photoelectron Spectroscopy (XPS).** XPS data were recorded on a VersaProbe I (PHI) System and high-resolution spectra were acquired applying a pass energy of 69 eV. The PHI MultiPak software was used for spectra analysis. All the deconvolution procedures have been performed after having shifted the C<sub>1s</sub> peak at 284.5 eV (in order to compensate for surface charging phenomena). Few

inorganic impurities were found (Na, K, Mg) but only organic compounds were taken into account for further examination in high resolution.

**Contact angle.** Water contact angles were measured by the sessile drop technique using a KSV-CAM 200 instrument. This technique gives information about the solid surface tension from contact angle of a liquid drop on a surface, according to the Young equation. This can be easily performed by establishing the tangent of the angle at the base, between the solid surface and the drop. Following the standard procedure, contact angle was measured to analyze wettability of polymer brushes. 4  $\mu\text{l}$  MilliQ ( $18\text{ M}\Omega\text{ cm}^{-1}$ ) water was dropped on polymer brush samples with 5.5  $\mu\text{l}/\text{sec}$  dispense rate.

**Biocompatibility assays.** NIH-3T3 fibroblasts were cultured in low glucose DMEM and incubated at 37 °C in a humidified atmosphere of 95% air and 5% CO<sub>2</sub>. Prior to cell seeding, azopolymer brush substrate was sterilized under UV light for 30 minutes. After 24 hours cells were fixed with 4% paraformaldehyde for 20 minutes and then imaged with a brightfield microscope and then stained for confocal imaging. Cells were permeabilised with 0.1% Triton X-100 in PBS for 3 minutes. Actin filaments were stained with TRITC-phalloidin. Samples were incubated for 30 minutes at room temperature in the phalloidin solution (dilution 1:200). Focal adhesions (FAs) were stained with vinculin. Briefly, cells were incubated in an anti-vinculin monoclonal antibody solution (dilution 1:200) for 2 hours and then marked with Alexa Fluor 488 conjugated goat anti-mouse antibody (dilution 1:1000) for 30 minutes at 20 °C. Finally, cells were incubated for 15 minutes at 37 °C in Hoechst solution to stain the cell nuclei. A LSM-510 confocal microscope (Carl Zeiss) was used to collect fluorescent images of cells on azopolymer films (Figure S9). The used laser lines were 488 nm (vinculin), 543 nm (actin) and 405 nm (nuclei).

**Fluorescence Correlation Spectroscopy (FCS).** One method to analyze the fluctuations in fluorescence intensity resulting from the azopolymer brushes is to calculate the temporal intensity autocorrelation function. In general, the autocorrelation analysis of fluctuations of fluorescence

intensity is known as Fluorescence Correlation Spectroscopy (FCS). Notice that all values reported in the main text of the manuscript refer to  $\tau_{diff}^R$ , therefore  $\tau_{diff} = \tau_{diff}^R$ .

In Figure S10 we report representative ACF curves measured when exciting azo-pMAb 1 with different wavelengths.

In Figure S13 we report representative CRs of azo-pMAb 2a obtained at two different excitation powers. A diverse fluctuation arises when the laser power substantially increases. As discussed in the main text and showed in Figure 3, the effect on the mobility of azo-pMAb 2a, when the laser intensity increases, is to substantially increase polymer mobility as well as the number of particles fluctuating within the confocal volume. The number of particles  $N$  is evaluated from the fitting of the ACF using Equation 2 and from the normalization over the overfilling of the objective through previously calibrated measurements in solution on Rhodamine 6G on the same optical path at different laser intensities, as reported in Figure S14.

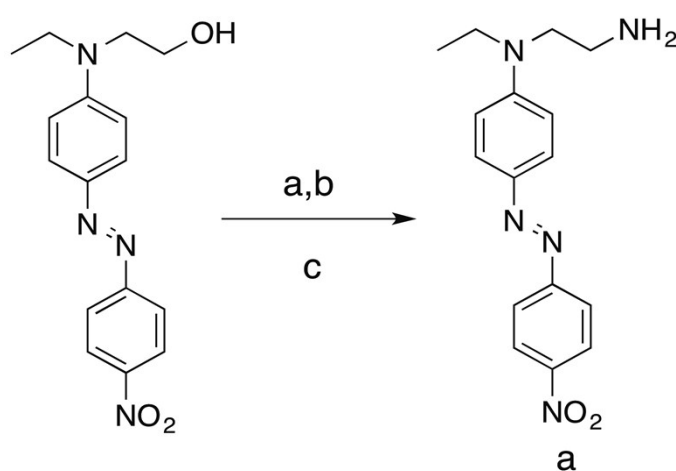
We show the comparison between the ACF plots of pMAb 3 (no azobenzene-containing polymers) and azo-pMAb 1 before being excited with 488 nm as shown in Figure S15. The two ACFs show very long decorrelation times (633 nm channel). When fit to Equation 2 and normalized to the same optical dimensions, it appears that pMAb 3 is showing a smaller diffusion time.

**Raman Spectroscopy.** The Raman spectra were excited with a diode laser at 532 nm with 20 mW maximum intensity on sample. A 50x /0.75 objective was utilized to focus the laser beam onto the 2D solid substrate. The investigated mapping area was chosen to be 221 x 459  $\mu\text{m}$  size with a step of 17  $\mu\text{m}$  between each point (351 total map points). The Raman spectra were acquired with a DXR Raman spectrometer from Thermo-Fischer Scientific at room temperature.

### Synthetic conditions and thickness of polymer brush samples.

Sample	Condition				Thickness *
	Time (h)	Temp. (°C)	Molar Ratio of RAFT and I with respect to M (8 mmol)	RAFT (%)	(nm)
A	6	70	0.054 mmol and 20.5 $\mu$ mol	100	150
B	11	70	0.054 mmol and 20.5 $\mu$ mol	100	200
C	6	70	0.027 mmol and 20.5 $\mu$ mol	50	160
D	6	70	0.038 mmol and 20.5 $\mu$ mol	70	170

**Table S1.** Synthesis of different poly(methacrylic acid) brushes prepared using different conditions to select the appropriate grafting density. (I stands for initiator, while M for monomer). (\*) Thickness was measured by ellipsometry.

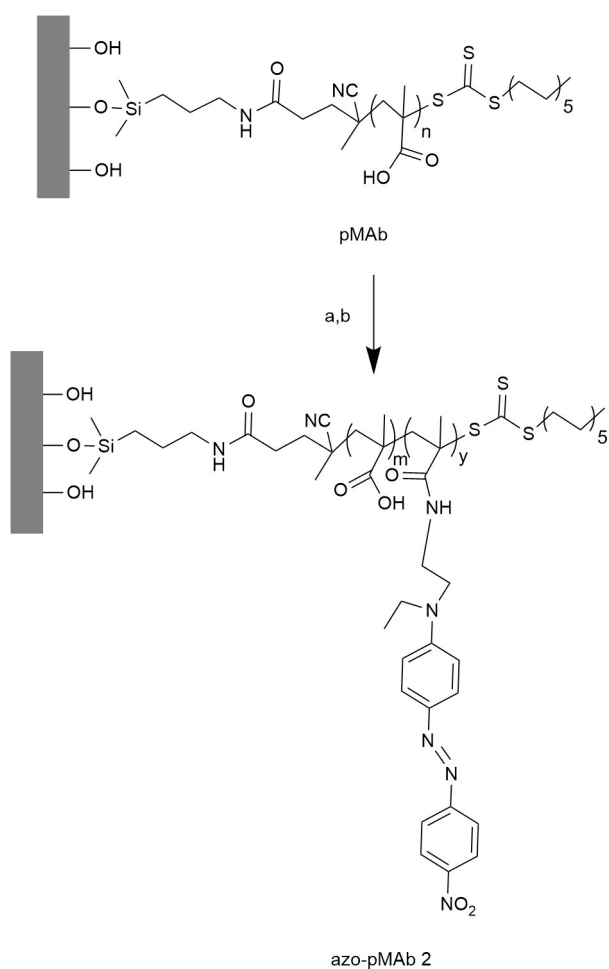


**Scheme S1.** Synthesis of DR-amine (compound **a** in this Scheme). Reagents and conditions. a) 2.4 equiv. of methanesulfonyl chloride, 3 equiv. of triethylamine in DCM at RT, b) 2 equiv. of sodium azide in DMF at 85 °C for 2 h and c) 1.5 equiv. of triphenylphosphine in THF/H<sub>2</sub>O (35/65, v/v) at RT for 24 h.

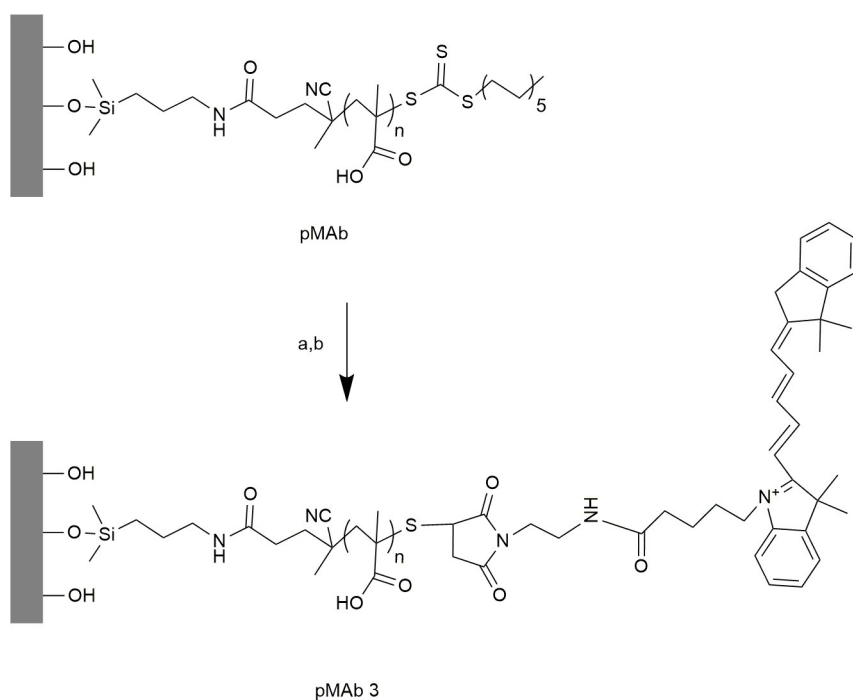


Samples	Time (h)	Grafted DR (%)
azo-pMAb 2a	6	4
azo-pMAb 2b (I)	12	70
azo-pMAb 2b (II)	24	70

**Table S2.** Conditions for azo-pMAb 2a and 2b. Conditions and grafted DR percentage are reported.



**Scheme S2.** Synthesis of azo-pMAb 2a and 2b. Reagents and conditions: a) 146  $\mu$ l of thionyl chloride in THF at RT for 12 h. b) In the case of azo-pMAb 2a: 626 mg DR-amine in DMF at RT for 6 h ( $y \sim 4\%$  that corresponds to the DR percentage in the polymer backbone). In the case of azo-pMAb 2b: same quantity of DR-amine in DMF at RT for 12 h ( $y \sim 70\%$ ).



**Scheme S3.** Synthesis of pMAb 3. Reagents and conditions: (a) 125  $\mu$ l of propylamine with respect to brushes in DMF at RT for 3h. b) 1 mg of maleimide-Cy5 in DMF at RT for 24 h.

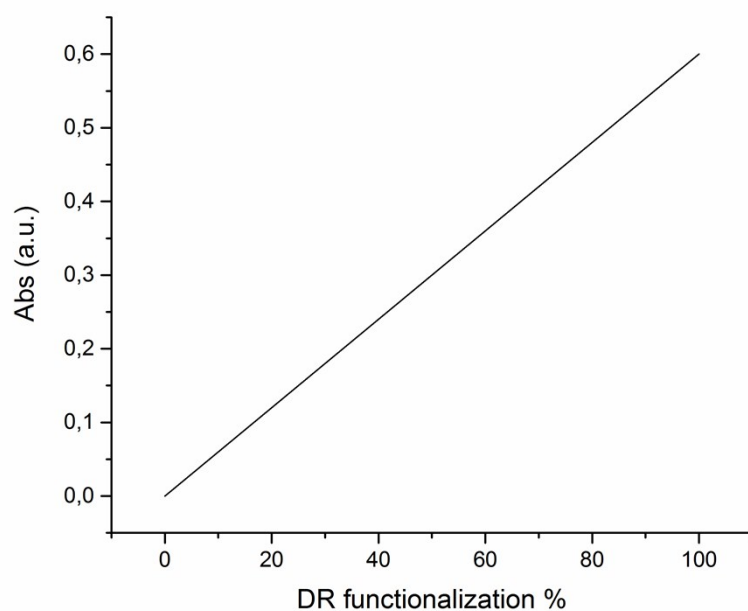


**Figure S1.** UV/Vis absorption calibration curve of DR-substituted pMAb samples. This curve has been obtained from the point at 0 absorption at 482 nm, which corresponds to the absence of DR molecules in sample pMAb and, and the point at 0.6 absorption, corresponding to a polymer brushes

sample obtained from the polymerisation of a DR-containing polymer brushes sample, thus 100% of DR functionalisation.

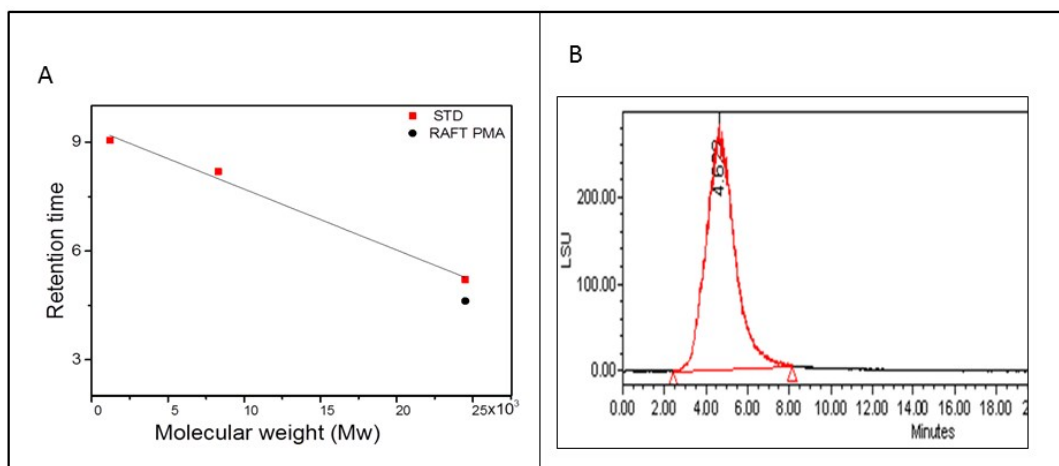


**Figure S2.** GPC chromatogram of non grafted polymer (pMA). (A) Graph of retention time versus estimated molecular weight. Red squares refer to commercially available poly(MA standards (MW were 2kDa, 7kDa and 25kDa, respectively), while black dot is referring to synthesised poly(MA by RAFT in solution condition C. (B) GPC chromatogram of synthesised poly(MA by RAFT in solution using condition C.

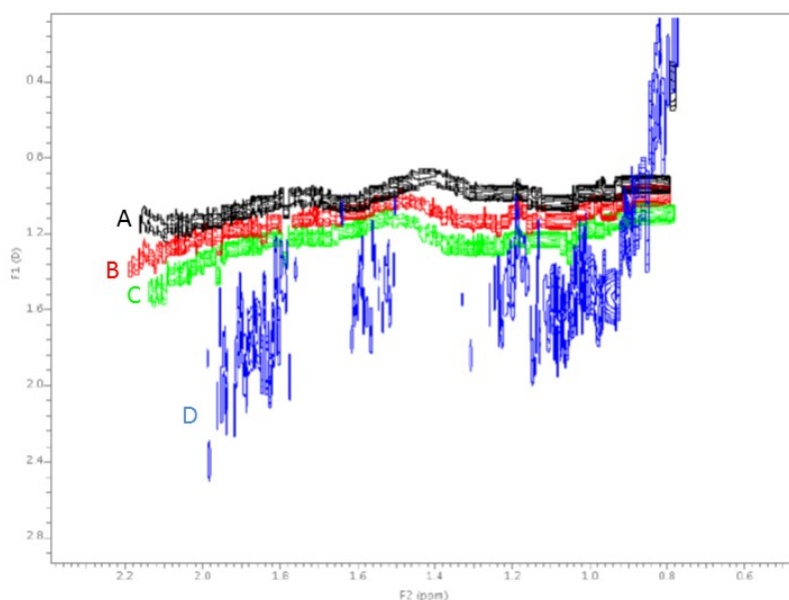


**Figure S3.** 2D DOSY NMR spectra of non grafted polymer (poly(MA)). Spectra of polymer samples prepared applying different synthetic conditions (samples A, B, C and D as reported in Table S1) were recorded in D<sub>2</sub>O at 300 K.

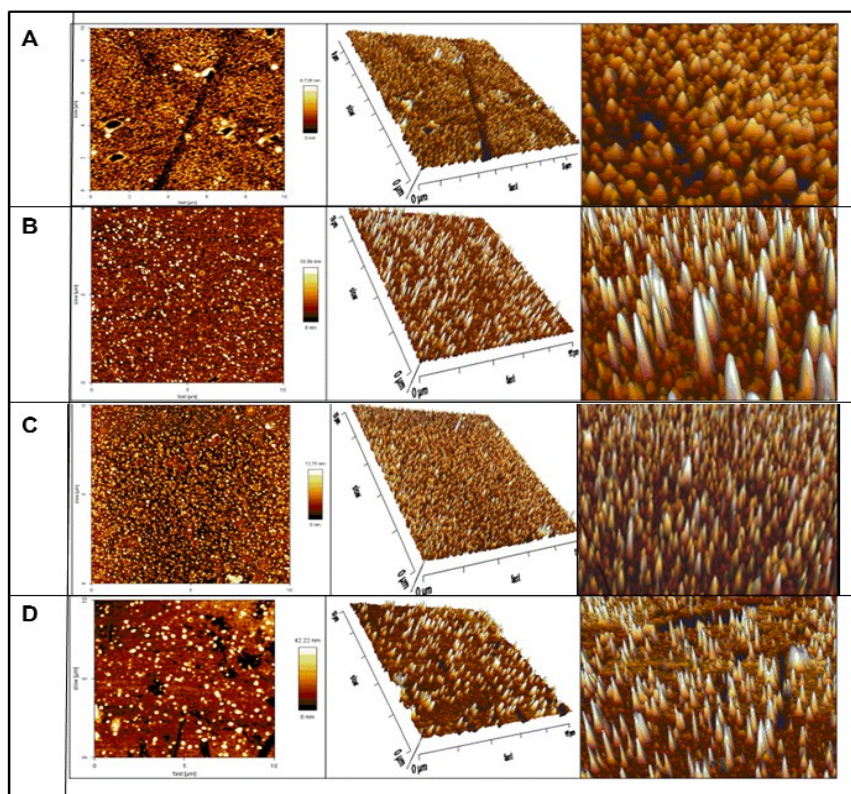


**Figure S4.** AFM images of pMAb samples synthesised in different conditions. Samples A, B, C and D. (Conditions are reported in Table S1).

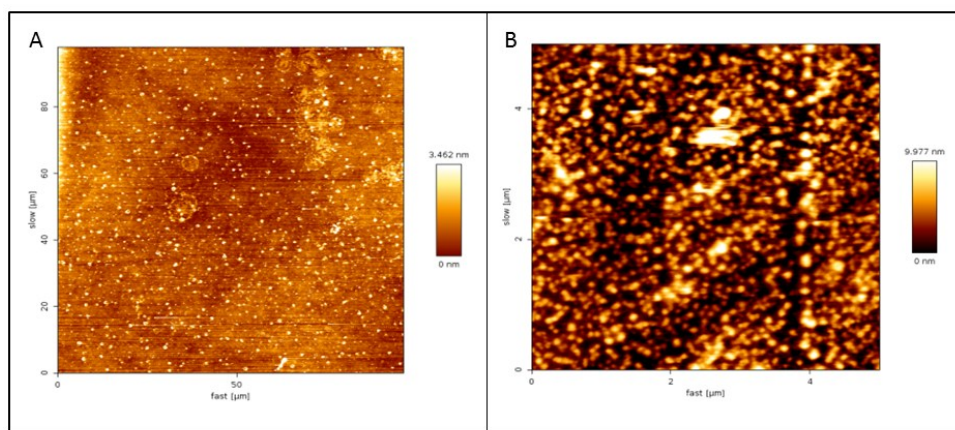


**Figure S5.** AFM images of (a) silanised glass and (b) RAFT immobilised on silanised glass.

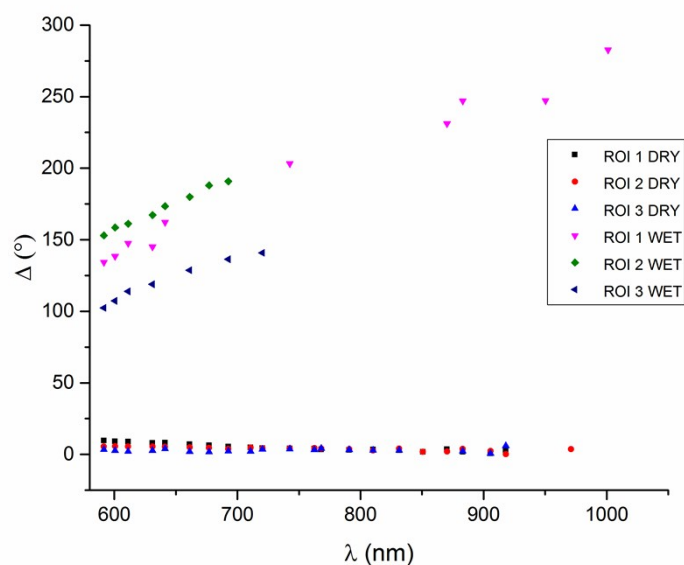


**Figure S6.** Spectroscopic ellipsometry raw data of azo-pMAb 1 in dry and in wet.

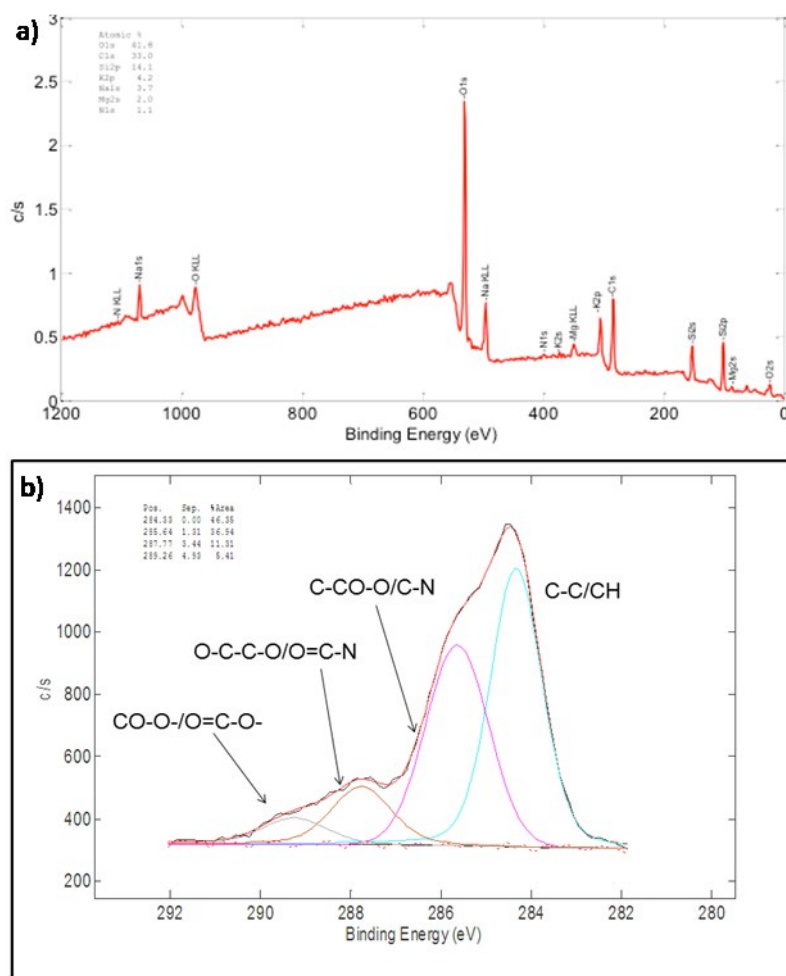


**Figure S7.** (a) Survey spectrum of pMAb. (b) High-resolution XPS spectra of the  $C_{1s}$  signals of p(MA) brushes (160 nm of thickness).

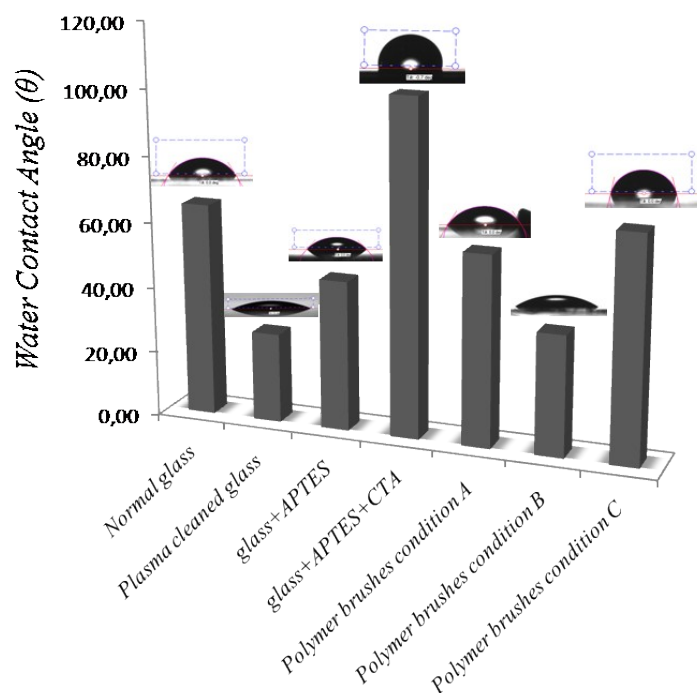


**Figure S8.** Contact angles of different samples: bare glass, plasma cleaned glass, silanised glass, RAFT immobilised glass and pMAb. Samples were prepared according to different polymeric conditions as summarized in Table S1.

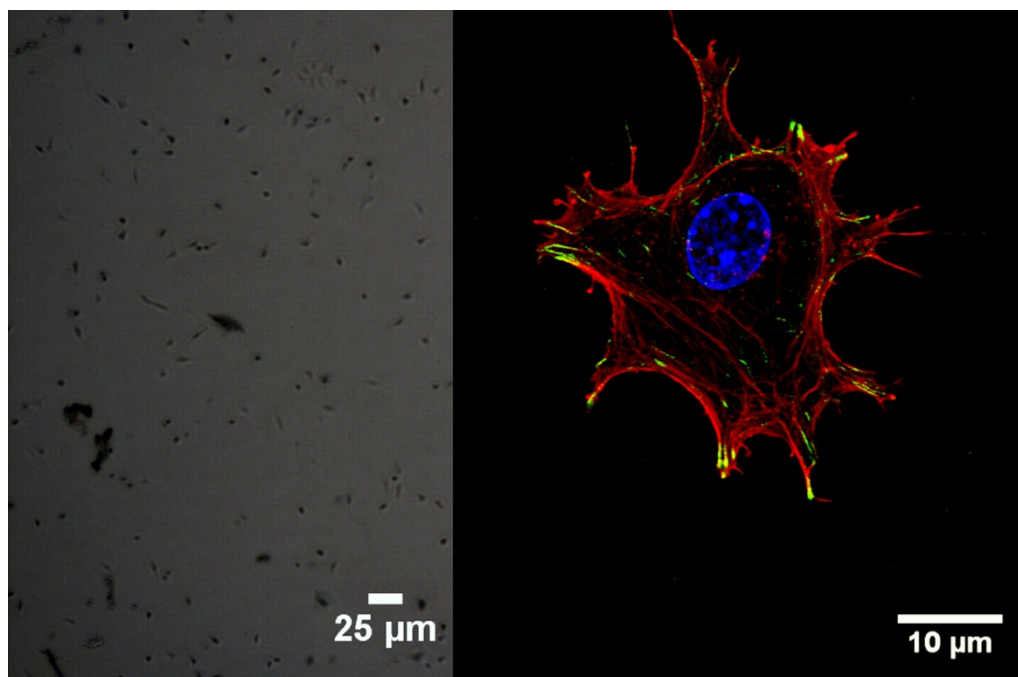


**Figure S9.** (a) Brightfield overview image and (b) confocal micrograph of a single NIH-3T3 cell on azo-pMAb 2a surface. Actin filaments were stained with TRITC-phalloidin (red),

focal adhesions were immunostained for vinculin (green) and nucleus was stained with hoechst (blue) after 24 h of incubation.

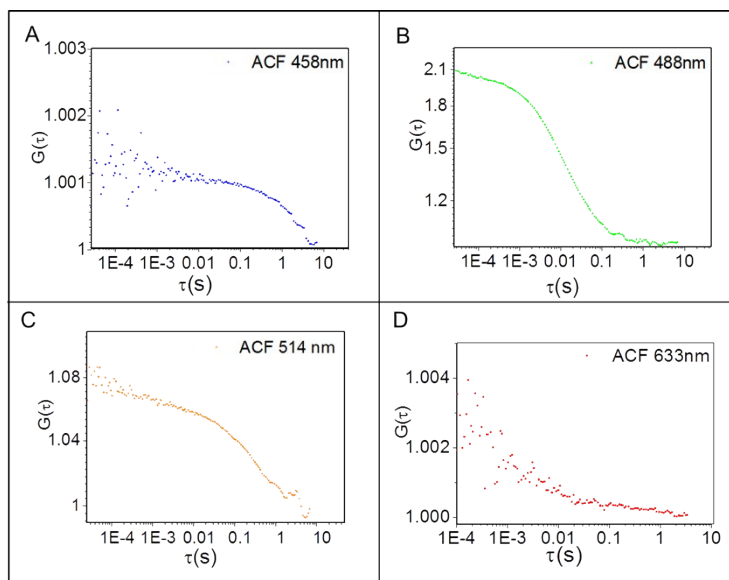


**Figure S10.** ACF plots of azo-pMAb 1 excited at different wavelengths: (A) 458 nm, (B) 488 nm, (C) 514 nm and (D) 633 nm, respectively.

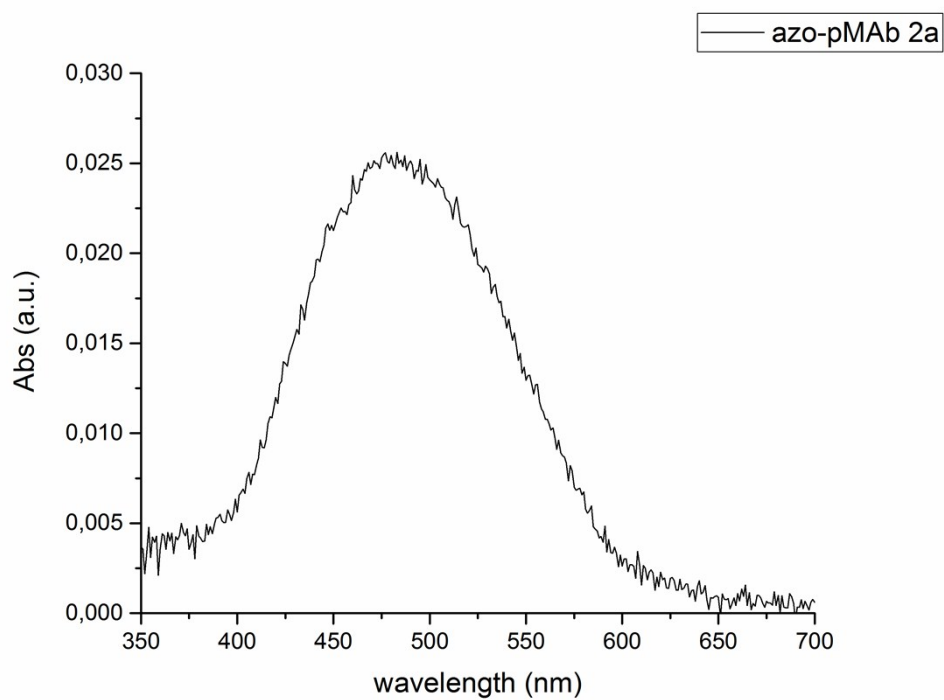


**Figure S11.** UV absorption of azo-pMAb 2a.



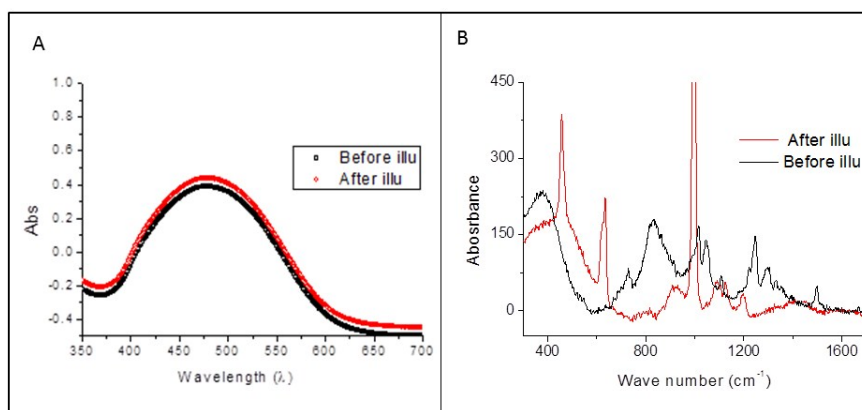


**Figure S12.** UV absorption and Raman spectra of azo-pMAb 2a. (a) UV spectra of azo-pMAb 2a (black line) before and (red line) after illumination. (b) Raman spectra of azo-pMAb 2a (wave number of 400-1700  $\text{cm}^{-1}$ ) before (black line) and after (red line) illumination during FCS experiments. In the latter case, the peak at 1012  $\text{cm}^{-1}$ , related to the phenyl rings of DR, drastically increased.

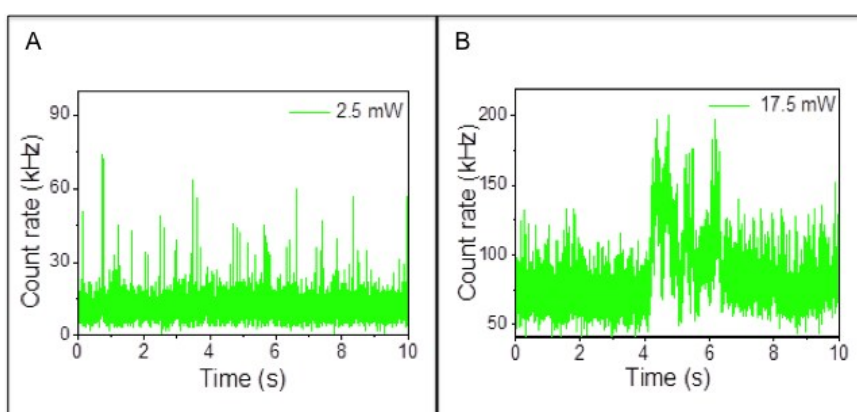


**Figure S13.** Count rates of azo-pMAb 2a excited with different laser powers and acquired in the 488 nm channel. (A) 2.5 mW and (B) 17.5 mW laser power, respectively.



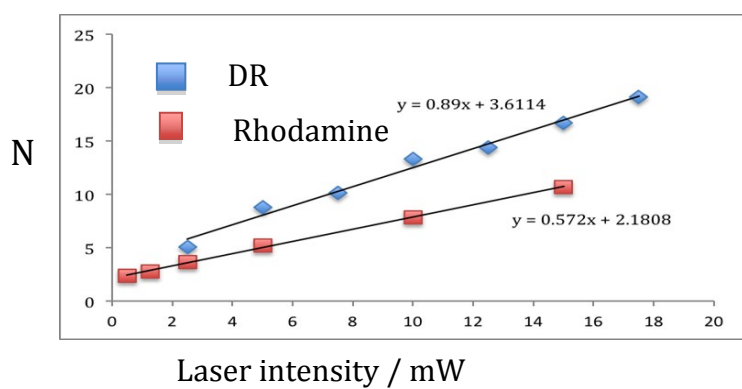


**Figure S14.** Number of molecules (N) evaluated for DR linked to azo-pMAb 2a and Rhodamine 6G in solution at various laser intensities of Argon 488 nm excitation, after fitting of ACF using Equation 2.

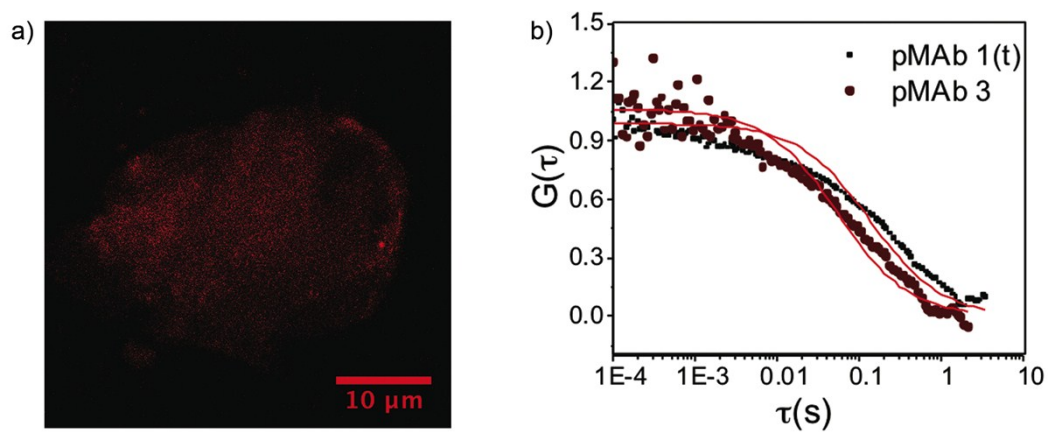


**Figure S15.** Confocal Image and ACFs of pMAb 3. (a). Comparison of the ACFs of azo-pMAb 1 before excitation (t) and of pMAb 3.